# HAM Relay-optics Suspension: pre-conceptual design LIGO-T1900036-v5

K.A. Strain, R. Jones

February 26, 2020

## 1 Introduction

This document presents initial design recommendations for the HAM relay-optics suspensions. A triple suspension is recommended to meet isolation requirements (see below), and the proposed name of HAM Relay-optics Triple Suspension (HRTS) remains appropriate. The sections below consider requirements, general desgin approaches, initial down select against requirements, details of selected design, and performance summary. The associated Solidworks models are presented in D1900032. Note that some of the details presented below are intended to match -v2 of the Solidworks model. Design-development notes, including FEA results, are provided as T1900088.

Reasons this report is considered preliminary include:

- interface requirements are incomplete in terms of both envelope and optical layout,
- the requirements of the suspension's support structure are unclear,
- the assembly process has not been considered in detail,
- as a result of the above, the mechanical design and hence MATLAB model may require to be reconsidered.

Steps have been taken to minimise the risk from the above, but it is accepted that the suspension support structure may require to be relatively complicated to meet all requirements for e.g. laser beam clearance and clear-access to inner parts during assembly.

## 2 References

## 2.1 Requirements

LIGO-T1800413-v1 HRTS requirements document

LIGO-T1800066 HAM table motion, basis of isolation requirements

LIGO-T1800042 Detector sensitivity goal, basis of isolation and noise requirements

LIGO-T0900496-v4 BOSEM noise measurement report (references requirements).

LIGO-E2000143-x0 HRTS PDR filecard.

## 2.2 Design ideas and precedents

LIGO-G1801998-v2 Preliminary design ideas for HRTS

LIGO-G1801990-v4 HRTS blade layouts and optical path through HAM3 to HAM6. This document has recently been updated to v5, which is now under consideration with respects to constraints on the HRTS.

#### 2.3 Models

LIGO-T080311-v4 HSTS MATLAB/Simulink suspension models.

These models were applied with some modification. For operational convenience, the triplep parameter file was included within the generate command. The important ssmake3MB function was used without non-trivial changes. A repository of the MATLAB and Simulink files is being prepared; to be stored within the DCC entry for the present document.

## 2.4 Revision changes

- -v2: additional material relating to the formal DRD/CDD requirements, reconcilliation of parameters with Solidworks model. Changes to mass and moments of inertia of top and intermediate masses intended to improve damping and increase margin for design changes new simulation results reflect revised design. Added a section covering magnet size for damping and alignment.
- -v4: mode frequencies, for comparison with 0.7 Hz lower limit in DRD.
- -v5 revision includes updates in response to HRTS PDR including new section on updated parameters, and updated m-file.

## 3 CDR checklist

This document sits in lieu of a formal CDD as defined in LIGO-M1500263-v1. At present it remains unclear how the reviews for the BHD subsystem are to be organised. The HRTS may form one element of a larger, sub-system review. The following table is included as a point of reference as to which areas within the topic of the HRTS, are covered by the current document. Notes

- a may also be captured in a BHD-subsystem CDD (TBC)
- 1 to be derived from HSTS hazard analysis E0900332, noting the present design is smaller, lighter and contains less stored energy
- 2 we are not sure where to find an example FMEA for a suspension, see below for an attempt
- 3 preliminary design is a responsibility of UK WP3.2, owned by RAL.
- 4 prototyping (UK WP3.2/RAL): it is proposed to build a prototype following FDR andfa prior to quantity procurement.

2

- 5 cost estimate: see UK proposal for cost envelope
- 6 see UK schedule or hooks to US schedule
- 7 TBC

Document	Section	Item	Notes
DRD		General performance requirements	a
DRD		Preliminary technical specifications	a
DRD		Requirements allocation	a
	4	Options analysis/ election	
	4 8	Data and trade studies	
	8	Hardware approaches satisfy defined function(s)	
	4	Draft hardware requirements	
		Interfaces identified	
		Hazard Analysis draft; personnel/equipment	1
		Draft Failure Modes and Effects Analysis	2
		Risk Registry items	
		Plans for the Preliminary Design phase	3
		Plans for prototyping and testing	4
		Cost estimate	5
		Schedule	6
		Review process documents	7

## 4 Fitting the design to requirements

We note that other requirements such as engineering standards, vacuum-compatible materials, etc. are assumed to be met unless otherwise stated, as in most cases the materials and techniques are similar to those previously employed in aLIGO suspensions. Exceptions include hard-drawn annealed stainless-steel wire, and martensitic stainless steel blade springs, both of which required to be reviewed at the appropriate point in time. Fall-back alternatives are music wire and maraging blades respectively.

The following requirements are considered to be the primary design drivers, in approximate order of consideration below:

Physical to fit in the space indicated on slide 10 of LIGO-G1801990-v4 (interpreted below)

Practical consider engineering techniques and materials that facilitate assembly and installation.

**Isolation** reduction of mirror motion relative to HAM table motion as defined in Figure 3 of LIGO-T1800413-v1 (reproduced below)

Noise filtering of BOSEM noise to meet requirements defined in Figures 1 and 2 of LIGO-T1800413-v1 (reproduced below)

**Damping** to provide approximately 10 s settling time to 2% in respect to a suspension point impulse.

#### 4.1 Physical

The volume available for the HRTS is much less than for the existing HSTS design. This is made clear on slide 10 of LIGO-G1801990-v4 (AKA slide 9 of G1801998), which presents an indicative envelope. The beam height at this location is 170 mm above the HAM table surface, and the top of the envelope is indicated at approximately 648 mm above the same surface. This provides 25.4 mm clearance to the sloping ceiling of the HAM chamber. Furthermore, due to the curved ceiling, with tangent at roughly 45 degrees at the closest approach of the suspension, keeping the suspension narrow, at least near the top, is likewise necessary. At this stage in development, it was thought to be important to define the suspended masses, blades, wires and

attachments, clamps and sensor-actuator (BOSEM) configurations accurately. As explained in the introduction, however, no serious attempt was made to design the supporting structure.

#### 4.2 Practical

Experience with suspensions with far sub-kg payload optics has been gained in 10 m prototype experiments in Glasgow and at the AEI. While by-and-large considerations scale from larger suspensions, areas of difficulty have been identified, and these were taken into account in the present work.

#### 4.2.1 Wires

Light masses require fine suspension wires. The most reliable and easily handled thin wire within our direct experience is 26 micron radius hard-drawn annealed stainless (304) medical wire type 304V, condition 'Hyten (min. 2932 Mpa)', finish 'SLT', produced by Fort-Wayne Metals. This has a similar strength to undamaged music wire, and does not require processing before handling, to reduce coiling and kinking. Experience, mainly at AEI-Hanover, indicates that it is much less likely to be damaged during handling than any other wire that was tested. This leads to far fewer breakages during assembly and installation, and its use should considerably accelerate assembly, balancing and installation of small suspensions. As this radius is the finest available within our experience, its use was assumed for the mirror-stage and taken to constrain the minimum acceptable mass of the payload at approximately 300 g: the mass of a 3-inch diameter fused-silica optic (76 mm) of thickness 30 mm. Wires in upper stage(s) may be thicker versions of the same material, or music wire. As these are in series with blade-springs, the wire may be somewhat thicker than required to support the load, and chosen to favour handling, clamp design, etc., for example, music wire of diameter of 4 mil (0.106 mm) may be suitable.

## 4.3 Blades

Small blades suitable for loads below about 1 kg, are difficult to manufacture with precision, particularly if made from maraging steel. The material typically has to be lapped to thickness, and this must be done without over-heating the steel. In this respect, grinding although quicker, does not yield a good result. Variation of mechanical properties within the sheet material, leads to a spread of blade stiffness and a requirement for matching blades into sets, or otherwise screening. Finally, it has been observed that some small maraging blades have failed in terms of robustness in handling – this is not fully understood. This experience, typically long lead-times and difficulties relating to corrosion led to consideration of an alternative grade of steel.

There is, unfortunately, a lack of clear creep data with respect to spring steels at low stress and low (room) temperature, almost all data relating to temperatures above 700° C and often at more than half of the ultimate tensile stress. Some indications of typical behaviour at lower stress were cited by Alessandro Bertolini of Nikhef, including 11499232. The suggestion being that certain fully-tempered spring steels, including martensitic stainless spring-steel, such as the commonly-used 410 series or similar, and the 440C grade employed in the VOPO suspensions (see below), are relatively free of creep. Given the modest requirements for isolation and noise (see below), light masses and overall design constraints, it is reasonable to consider flat, blades laser-cut from suitable steel sheet and with a design stress under load of approximately 400 Mpa. These blades can be cut from precision sheet that is readily available in suitable thicknesses: i.e. 500 and  $1000 \,\mu\text{m}$ . The resulting blades are are corrosion resistant and the cost is a few percent of maraging blades of similar dimensions. Other advantages include the option of complex shapes

available from laser cutting and very rapid production cycles (days rather than months). If other grades of steel are recommended these would be considered.

Apart from size, the proposed blades are broadly similar to those of the VOPO Isolation tables LIGO-E1600165-v1, and are employed in a 'bent when loaded' configuration. The dimensions of the blades are discussed below. It may be noted that the maximum isolation set by requirements exists at a frequency only a few times higher than the resonant frequency of the loaded blades, and this eases blade design (considerations of internal modes, centre-of-percussion effects and other non-ideal behaviour are not expected to be important. This is based on experience and is to be confirmed by FEA in due course). The precise grade of steel remains to be selected. As an interim measure prototype blades were obtained and are held at Glasgow available to be characterised. Note that all of the materials under consideration are somewhat magnetic.

These 'bent when loaded' blades require angled clamps – it may be necessary to allow a 'library of clamps' that may be selected from to match the available blades.

Note that, should a problem arise with stainless blades, the fall-back would be to choose maraging blades. Although, in principle, maraging blades could be made smaller than the stainless ones, this is not recommended given the previously observed problems with such blades. If maraging blades were chosen, particular attention would be paid regarding the stress produced at the 'neck' by loads during assembly, and to protection against corrosion prior to installation in vacuum.

## 4.4 Pitch alignment

Small suspensions, with fine wires that are hard to handle, suffer from imbalance resulting from tolerance build-up between front and rear wires, clamps and break-offs. To reduce this effect, the wire-connection-point offsets (from centres-of-mass) in the vertical and longitudinal directions (i.e. d and s offsets in the MATLAB model) were kept at or above 2 mm. Further, the design of the upper mass allows moveable slugs to assist balancing. The option of balancing slugs at the intermediate mass remains to be considered.

## 4.5 Physical access for assembly and adjustment

Where small suspensions are optimised only for dynamical behaviour, it is likely that some adjustments or assembly steps become rather intricate. This is to be avoided in the HRTS which require to be produced in a relatively large quantity. Some of the design constraints arise from consideration of access for assembly, inspection and adjustment.

#### 4.6 Isolation – the requirement for a triple suspension

The isolation requirements given in Figure 3 of T1800413 were reproduced in MATLAB to allow comparison with suspension models. It was observed that, for any of the options under consideration that may fit within the available envelope, the key requirements are horizontal isolation in the frequency range around 12-14 Hz – if met there the requirements would be exceeded at all higher frequencies. Likewise for vertical isolation, if the requirement is met at around 15 Hz, it would be met at all higher frequencies – except, perhaps, around 30 Hz which could be significant in a design with one set of blade springs – and that is seen to be ruled out in any case.

To simulate double-suspension options rapidly, the triple suspension model, was altered by setting the middle stage to be short and light. This allowed *approximate* double-suspension transfer functions to be obtained. If the double-suspension design was to be developed further, a proper double-suspension model would be required to remove errors at the sub-percent level.

Vertical and longitudinal isolation are considered separately.

## 4.6.1 Vertical isolation – how many blade-spring layers are required

Constraints: top-stage blade length is constrained by the suspension envelope and by the need to avoid blades that are too long and thin. Even allowing for overlapping/crossing blades – see renderings in LIGO-G1801998-v2, 150 mm blade-length is taken as a practical limit. The length of the blades within the top mass is limited according to a fairly complex set of constraints arising from suspension dynamics and damping. Essentially, the moment of inertia of the top-stage, around the vertical axis, cannot be too-much larger than that of the second stage, although other factors come into play albeit at a more subtle level in their effect. There is also a direct effect on the envelope if the top mass becomes too wide. These constraints led to consideration of blades in the second stage of length in the range from 65 mm to 80 mm.

With these constraints, one stage of vertical isolation from blade-springs fails to meet the isolation requirement between around 12 Hz and 50 Hz. Meeting the requirement would require reducing the vertical mode frequency of the spring stage to below 1 Hz, while ensuring the blades would be robust and provide near-ideal transmissibility up to at least 20 Hz, something that is considered to be impractical given the requirement for compactness.

It would in principle be possible to construct a double-suspension with two spring stages, i.e with the payload mass wires connected to the top-mass blade springs. This arrangement would result in essentially the same vertical isolation as the triple suspension case described below, and so the decision of whether this design has merit depends mainly on the evaluation of horizontal isolation.

## 4.6.2 Horizontal (longitudinal) isolation – double or triple suspension

Constraints: the total height-budget for the suspension chain, measured from the blades at the top to the centre of the payload, as derived from information stated above, is in the region of 430 mm. This could be a double suspension of around 160 mm and 250 mm stage length, allowing another cm or two for offsets, clamps etc., or alternatively three stages of roughly 115 mm, 115 mm, and 160 mm to form a triple suspension. Larger ratios between/among stage lengths would not provide better isolation. The double-suspension option is ruled out by the isolation requirements between 12 and 20 Hz approximately, and by as much as an order of magnitude at the maxima in the requirements around 13 Hz.

The triple suspension meets requirements and is the option taken forward.

#### 4.7 Noise

At this stage of the design process, relatively crude active local control filters have been assumed. These filters are defined in the 'DoF' space, and consist of a zero and pole below and above, respectively, the range of relevant mode frequencies. In the case of the longitudinal coordinate, a modest degree of low-pass filtering – a 2nd order section with pair of poles and pair of zeros – is included to meet noise requirements at around 11 Hz. It is assumed that there are two BOSEMs sensing and acting on longitudinal and vertical DoFs, therefore reducing the effective sensing noise by 3 dB relative to a single BOSEM sensor.

#### 4.8 Damping

Noting again the point regarding relatively crude local damping filters, it was considered how to adjust the parameters of the suspension to provide good visibility and control authority at the top mass for all relevant rigid body modes. For the translation DoFs, given the tightly-constrained stage lengths in the triple pendulum, and constraints on blade dimensions, this is achieved by choosing stage-masses relative to the target 300 g payload. The top mass turns out to be approximately 700 g (output from the Solidworks model of a reasonable design), and the intermediate mass may be from roughly 300 g to somewhat over 700 g while maintaining good coupling for the translation DoFs. As the intermediate mass increases it is necessary to stiffen the blades by adding width and/or thickness.

For the rotation DoFs, and given the choice of stage-masses, the moments of inertia result from the geometry of the various masses. The two lower stages were originally considered to be right circular cylinders with attachments such as break-offs and clamps. The payload mass is fused-silica. The intermediate mass was revised to provide more space for assembly and is presently considered to be made from steel with a large central void or voids. Subsequently more clearance above and below the intermediate mass was obtained by truncating it vertically – see also notes about pitch coupling, below. It was decided to follow the 'cross top-mass' approach that has been explored in 100 g-scale suspensions over the past decade. This approach was developed by the authors working with a series of students at Glasgow and later AEI (J. MacArthur, N. Gordon, and others). The 'cross' approach allows improved distribution of pitch moment of inertia, provides locations for magnets/flags to be attached for pitch sensing control, and includes space within the mass for adjustable pitch-balancing masses.

The details of the optimisation of the various suspension parameters are not given, other than to note the few that seemed most significant, and their relationship to the design outcomes.

## 4.9 Mode frequencies

The design requirements state that all modes should be above 0.7 Hz, to benefit from HAM table isolation. The lowest modes per degree of freedom, or coupled pair of degrees of freedom, obtained from the MATLAB model are as follows. For longitudinal and pitch, the lowest mode is at 1.00 Hz, is mainly longitudinal, and not strongly dependent on the degree of damping, with the suggested controller. For transvere horizontal and roll, the lowest mode is at 1.02 Hz, is mainly transverse, and not strongly dependent on the degree of damping, with the suggested controller. For vertical, the lowest mode is at 2.65 Hz (sensitive to blade stiffness). For yaw, the lowest mode at 0.74 Hz is easy to damp. With the suggested controller damping the second yaw mode at 2.13 Hz tends to damp the lowest mode quite strongly, and push up the peak to about 0.9 Hz. Yaw damping should be revisited when final moments of inertia are known, for the top and intermediate masses.

### 4.9.1 'd' values

As noted above, it was desired to avoid too-small  $\tt d$  values particularly at the lower stages. Further, to provide access to top-mass clamps and blade-clamps for the wires going upward and downward from that stage, these clamps are separated by 10 mm in the vertical direction:  $\tt d = 5\,mm$  for both. The cascade of  $\tt d$  values down to  $2\,mm$  at the payload was found to work well.

#### 4.9.2 's' values

The longitudinal offsets in connection points were chosen to accommodate reasonable clamp designs, and avoid wires at the intermediate stage being too close in proximity.

#### 4.9.3 'n' values

The transverse offsets of connection points were chosen to balance yaw-mode dynamics, with practicalities of construction. The value of n0 affects blade overlap and hence suspension envelope at the top. The quantities n1 and n2 affect top-mass design, as space is required to provide access to clamps, mount blades, etc. The remaining values are determined by the payload diameter taking account of break-offs.

## 4.9.4 Yaw dynamics

A limitation was encountered in the development of the HRTS in relationship to coupling of yaw modes – this turns out to be the most critical aspect of the dynamics problem. The top-mass is wide, in the transverse direction, compared to the lower stages, and good coupling of yaw motion of those lower stages to the top mass relies on suitable choice of certain parameters.

For the top mass, the yaw moment of inertia I1z requires to be limited (the notation for this is taken from the MATLAB models, in Solidworks it would be I1zz). This necessitated removal of 'excess' material at the transverse extremes of the mass, shortening of the blade springs to a minimum and other changes of mass distribution.

For the intermediate mass, the yaw moment of inertia I2z had to be increased. The starting point was a solid aluminium mass of around 3-inch diameter, this proved to have too little moment of inertia for good coupling. Changing to a steel mass with voids produced a better outcome given the expected range of value of I1z.

If I1z is later increased by more than about 10%, I2z is likely also to require to be increased in approximate proportion. This is likely to affect the total load on the blade-spring stages and therefore require minor revision of blade design.

Other parameters such as wire angles (n values), make less significant differences to yaw coupling, within the range of values that fit other constraints.

While similar concerns exist with roll, these drive the design to a lesser extent. Note that for both yaw and roll, the approach taken was to vary parameters until adequate damping could be achieved using the relatively simple local control filters outlined above. This led to the situation that the settling times for the rotation DoFs are dominated by the 'middle-frequency' mode.

Update for -v2: the mass and moments of inertia of the intermediate mass were increased, and those of the top mass decreased to provide better coupling. This was done to an extent beyond that necessary to obtain adequete performance, to provide margin for increases in top-mass moments of inertia during the detail design phase.

## 4.9.5 Bounce mode

The short lowest stage and the mass/wire-diameter constraints set out above, yield a bounce mode of 37.1 Hz. If left un-damped the isolation requirements would not be met in a 1 Hz band around this frequency, and affecting a slightly wider band given the expected spread among the many such modes per detector. It is assumed that a resonant damper should, therefore, be specified at the intermediate mass stage to damp these modes. Note that the slightly higher-than-usual frequency of the bounce modes is perhaps an advantage, overall, in this context. This requires further consideration – it is a feature of all broadly similar suspension designs.

Update for -v2: it is assummed that the required bounce mode damper can be fitted within the intermediate mass, the detail of the mass can easily be varied to accommodate a damper without significant changes to its total mass.

It is unknown whether roll-mode coupling requires similar consideration of damping for the roll

# 5 Initial estimate of magnet size assuming standard BOSEM coils

BOSEM actuators, in conjunction with typically 10 mm diameter magnets, up to 10 mm long, are employed to provide alignment of large suspensions including aLIGO quads. The HRTS are much lighter, and it would be expected that smaller magnets suffice. Pending decisions on the BHD/ISC/alignment and requirements, it is useful to have an initial, rough estimate of the magnet size that may be appropriate. It is noted that the mass of the magnet/flag assembly is important with regard to the moments of inertia of the top mass, motivating the choice of small magnets.

The 'cross' top-mass design provides approximately equal lever-arms and equal number of BOSEMs acting in pitch and yaw. The suspensions are considerably stiffer in pitch, however, and the relevant angular stiffness is  $\approx 0.28 \, \mathrm{rad/N}$  (assuming two 'pitch' BOSEMs each 0.06 m from the central axis). For an adjustment range of, say,  $\pm 5 \, \mathrm{mrad}$ , therefore, the required force per actuator is 17 mN. With the standard BOSEM coil, this peak force is produced at the standard maximum current of 200 mA. Therefore the actuator coefficient should be around 0.09 N/A, compared to about 1.7 N/A for the standard 10 mm diameter by 10 mm long magnets. Mark Barton's Sweetspot.nb Mathematica notebook, suggests 0.09 N/A is obtained with magnets 6 mm long and 3 mm diameter. Alternative shapes include 4 mm long and 4 mm diameter, providing a coefficient of 0.11 N/A, or even 5 mm long and 4 mm diameter, providing a coefficient of 0.14 N/A. The mass of the largest option is about 0.5 g.

## 6 Initial FMEA

The HRTS carries generally similar modes of failures to those that would be associated with the HSTS. Here we consider one further area of risk, associated with the use of thinner wires to support the lowest mass (i.e. 50 vs. 120-micron diameter). Such thin wire can be relatively fragile and susceptible to damage during assembly, adjustment and installation. If standard music wire were to be used, there would be substantial risk of kinking or similar damage during handling, leading to weakened wires and later failure, e.g. in an earthquake or table quake.

Mitigation — step 1: Fort-Wayne Metals (FWM) annealed and surface-hardened wire is specified for the lowest stage of the suspension, see section 4.2.1. This wire has similar ultimate tensile strength to music wire, but is far more robust in general handling. Experience with 50-micron wire of conventional (music wire) and FWM wire in the same context at the AEI-Hannover prototype, shows:

- the wire does not coil badly when removed from the spool easing handling and reducing the rate of damage during assembly to close to zero
- the wire does not require to be annealed during assembly (the usual cure for coiling)
- failures during assembly at the AEI prototype have been eliminated, or at least markedly reduced (small number statistics apply)
- there has been a marked reduction in suspension failures due to table quakes (from all of one kind of suspension, to no failures, including when both types of wire were in similar suspensions on the same table at the time of a quake, again small-number statistics apply)

Mitigation — step 2: include a proof test in the process whereby lower-stage wire loops are assembled, i.e. test with well-defined over-load after the wire clamps are attached. The protocol for this is to be determined before PDR. Note that the wires are stressed to about 350 MPa, assuming  $26 \,\mu\text{m}$  radius, as seen in the wire batch procured at AEI. The FWM quote to AEI lists an UTS of 2.9(32) Gpa, in line with ASTM A-228M-07 music wire.

# 7 Reasoning in support of the proposal of flat (not pre-curved) martensitic stainless steel blades

This section provides initial thoughts. It is proposed to develop these and carry out suitable tests of prototype blades during the preliminary design phase, with down-selection to the recommended blade design at PDR.

## Arguments against maraging/pre-curved maraging-steel blades:

Small maraging-steel blades, in particular those used in the AEI prototype 100g suspension, have not been very successful. While design changes and perhaps sourcing higher-quality material or otherwise improving production could help, the problems described below motivate consideration of alternatives that might allow easier and more reliable assembly of 10+ suspensions. Note that it is not proposed to consider pre-curved martensitic or other stainless blades as this would lose the processing simplicity and negate the low cost and ready availability of precision-cut springs. Even with lapping to thickness, initial matching of the small blades for the 100 g suspension (smaller than the top blades, but similar to the lower blades of the HRTS), was poorer than hoped for. Several of the blades were also damaged in handling, it is not clear at which point in the preparation and assembly process this occurred. Possibly, precipitation hardening did not achieve the desired properties uniformly throughout the blade, and especially near the "neck" of the blades, or possibly the stress of handling (i.e. tightening clamp-screws, or loading and flattening), was too great. The damage may have been due to torsion rather than the design load. One hypothesis is that the 1mm thick sheet all these blades were lapped and cut has poor homogeneity. Alternatively, perhaps the heat of working the metal has caused the later hardening process to be patchy in some sense. The point is that production of a well-matched set of small, pre-curved maraging-steel blades is not a solved problem.

These blades are also expensive (£300-£600) and the production cycle is inconvenietly long (typically 15-26 weeks, usually closer to the latter). There's the usual corrosion problem requiring plating, and then the hydrogen embrittlement problem.

#### Arguments for flat martensitic stainless steel blades:

The HRTS noise requirements are modest, the vertical transmissibility requirement can be met with two sets of blades with low-stress ( $\sim 400\,\mathrm{Mpa}$ ). The blades can be short, such that their internal modes are high ( $\gg 200\,\mathrm{Hz}$ ). The shape is then less critical: there can be extra material to bolster the strength at the neck at the expense of internal mode frequencies. The neck can, therefore, be thicker for better lateral and torsional stiffness (FE work is needed to optimise this, and RJ has started to look at this, initial sketches are designed instinctively based on the previously-observed weak points).

The sag of these blades under load is small (1.5cm for the lower and 2.5cm for the upper blades), and the difference between bent and flat blades is also small. Because of the shape of the ceiling in the HAMs, the place where the blades bulge up is not important in regard to vertical clearance.

It is proposed to select the blade material from martensitic stainless steel (of a grade TBD). The selected grade will be readily available in tempered, precision-rolled sheet, which can be laser cut with its temper retained. Based on intial samples, not necessarily of the final material, the

production time can be short and the cost can be expected to be much lower than for maraging blades. The VOPO suspension has flat stainless-steel blades, made from a martensitic material (440C) so we have some degree of precedent – see page 18 of E1600165.

Design document T1900088 reports initial FEA that was used to set the peak stress at about 400 Mpa. This stress is thought to be far below the region of concern, but this point requires further investigation prior to committing to this type of steel. Most information regarding creep comes from measurements at far higher stress (1 GPa) and usually also at high temperatures (800 C). Tests may be required to validate the choice of material.

It is expected that the stainless steel blades should be able to be very closely matched, and probably eliminate the need for adjustable blade clamps, requiring at most, a library of clamps within a narrow range. If this works out the main advantage is a substantial reduction in the assembly time for these 10+ suspensions (the same reason that the FWM wire is better).

## 8 Summary of performance measures

The MATLAB/Simulink models were exercised to produce the following results.

#### 8.1 Isolation

An m-file was created to reproduce the requirements shown in Figure 3 of T1800413. This was done by importing data from T1800042 and T1800066:HAM5\\_ref\\_curvesv1 in the useful and overlapping range between 9 Hz and 60 Hz. Interpolation was employed to bring the data to a common frequency axis. A scaling factor was introduced (as in T1800413) to account for the relative sensitivity of relay-optics mirrors relative to the detector-level requirement in T1800042. The results are shown in Figure 1 along with estimates of the isolation provided by the HRTS.

### 8.2 Noise

The m-file employed in the previous section could also be used to generate requirements for feed-through of BOSEM noise to the payload masses. This was considered for all DoFs, and is presented in Figure 2 for longitudinal and vertical frequency range for which the requirements are defined. For the present, it is assumed that there are two BOSEMs sensing each of these DoFs, leading to a 3 dB reduction in BOSEM noise, i.e. equivalent to a single-sensor with noise of no more than  $7 \times 10^{-11} \, \text{m/yHz}$  at 10 Hz and above. The comparison has been couched in terms of the combined mechanical and electrical gain/filtering necessary to meet requirements.

## 8.3 Damping

Longitudinal and transverse-horizontal damping provide settling times (to 2%) that are beyond the 10 s target <sup>1</sup>. Improved loop design should help to reach the target if required. Pitch and yaw damping appear to be adequate provided that moments of inertia of the upper two masses are close to design values as discussed above. The middle-frequency roll mode is not particularly well coupled to the top mass, this may be reconsidered given more accurate values of the relevant moments of inertia for the upper two masses. For convenience of scaling and clarity, the impulse responses for translation and rotation DoFs are shown in Figures 3, and 4.

<sup>&</sup>lt;sup>1</sup>Note that this target is stricter than the previous target of 10 s to 1/e. This choice was made a) to introduce margin, b) in lieu of a separate restriction on the Q of the middle mode, and c) as these suspensions should not add to the acquistion time for the detector as a whole

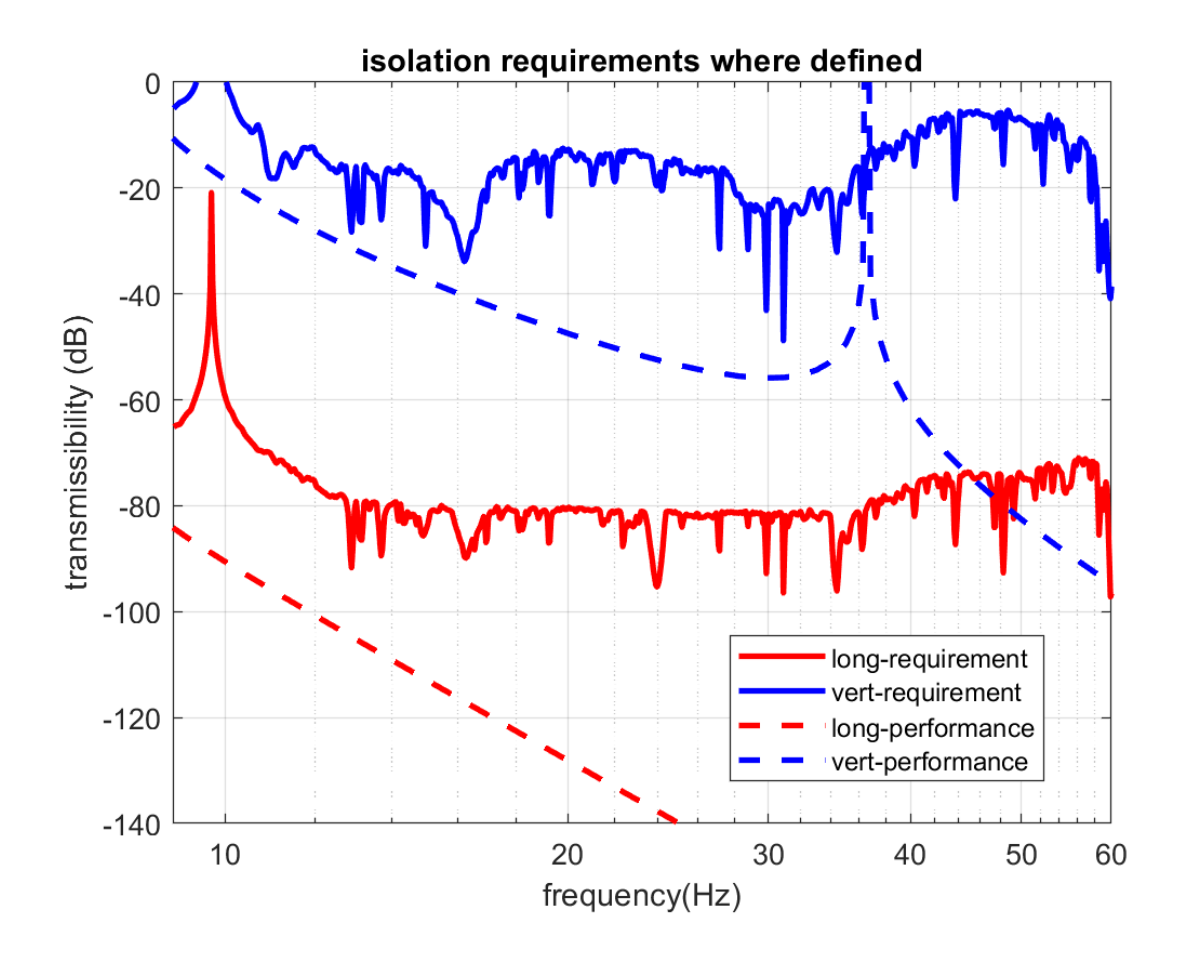


Figure 1: The blue (vertical) and red (longitudinal) curves represent the isolation requirements first stated in T1800413. The purple (vertical) and green (longitudinal) transmissibility estimates are seen to fall within the requirements. The exception being the narrow range around the bounce mode at 37.1 Hz, as noted in the text above. Damping of the bounce mode to  $Q \sim 100$  would meet requirements. We note that the requirements are only clearly defined within the frequency range shown.

# 9 Checks on damping performance during HRTS PDR

See LIGO-E2000143-x0.

Record of email sent on February 25th 2020, following a check of the above performance measures with new top and intermediate mass parameters (see dated comments in m-file below).

Mode frequencies are, as discussed last week, all above 0.7 Hz. The only mode below 1 Hz is the lowest yaw mode at 0.74 Hz. This is easy to damp and with the controller, is pushed up to 0.9 Hz, with very low Q. The next mode up is the 1 Hz longitudinal mode.

Even though the example controller is not sophisticated, the setting time in response to test impulses is short (not more than 22 s to 2%, or around 5 s to 1/e).

The refinements of the design of intermediate and top masses and correction of errors for the former, lead to

- no observable change in translational degrees of freedom (masses almost unchanged)
- Roll: (increased intermediate mass MI) the current value performs better than the original, indeed going even higher is also fine (e.g. I tried +25%).

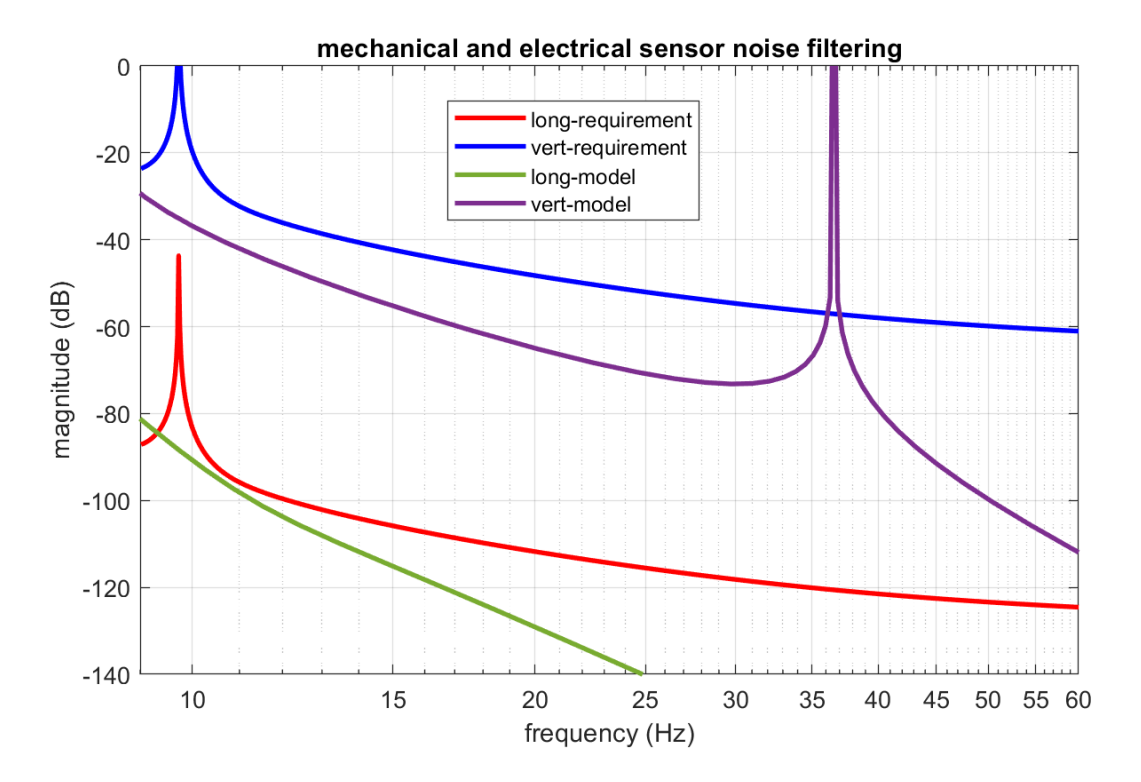


Figure 2: The blue (vertical) and red (longitudinal) curves represent the noise-filtering requirements derived from Figures 1 and 2 of T1800413. The purple (vertical) and green (longitudinal) transfer function estimates are seen to fall within the requirements. The exception being the narrow range around the bounce mode at 37.1 Hz, as noted in the text above. Note that to meet the longitudinal requirement, it was necessary to apply a low-pass filter with complex poles at 7.5 Hz and complex zeros at 12 Hz. As with other aspects of the local damping, this has not been optimised.

- Pitch: (decreased intermediate mass MI) there's substantial margin to adjust this ( $\pm 30\%$  tried).
- Yaw: The current value of intermediate mass MI seems to be about optimum (to match the top mass) increasing or reducing the MI by 15% leads to degraded damping, by about the same amount.

We should keep checking yaw and roll behaviour if there are further changes.

# 10 The MATLAB/Simulink model

The core of the model is an largely-unmodified <code>ssmake3MB</code> file from the HSTS design archive. This function is called from a combined <code>generate\_HRTS</code> file that contains the suspension parameters, defines local damping filters by calling six appropriate functions <code>local1</code> for <code>x</code> to <code>local6</code> for roll, and includes related factors such as <code>sensor/actuator</code> offsets or 'lever-arms' and overall gain values. Most of this script is reproduced below as a means of listing the suspension parameters for cross-checking against the Solidworks model. Note that the 'lever-arm' values as with all aspects of the local damping, are preliminary, and of little consequence given the assumption of DoF damping.

A Simulink diagram was produced to represent the suspension and controls, with appropriate

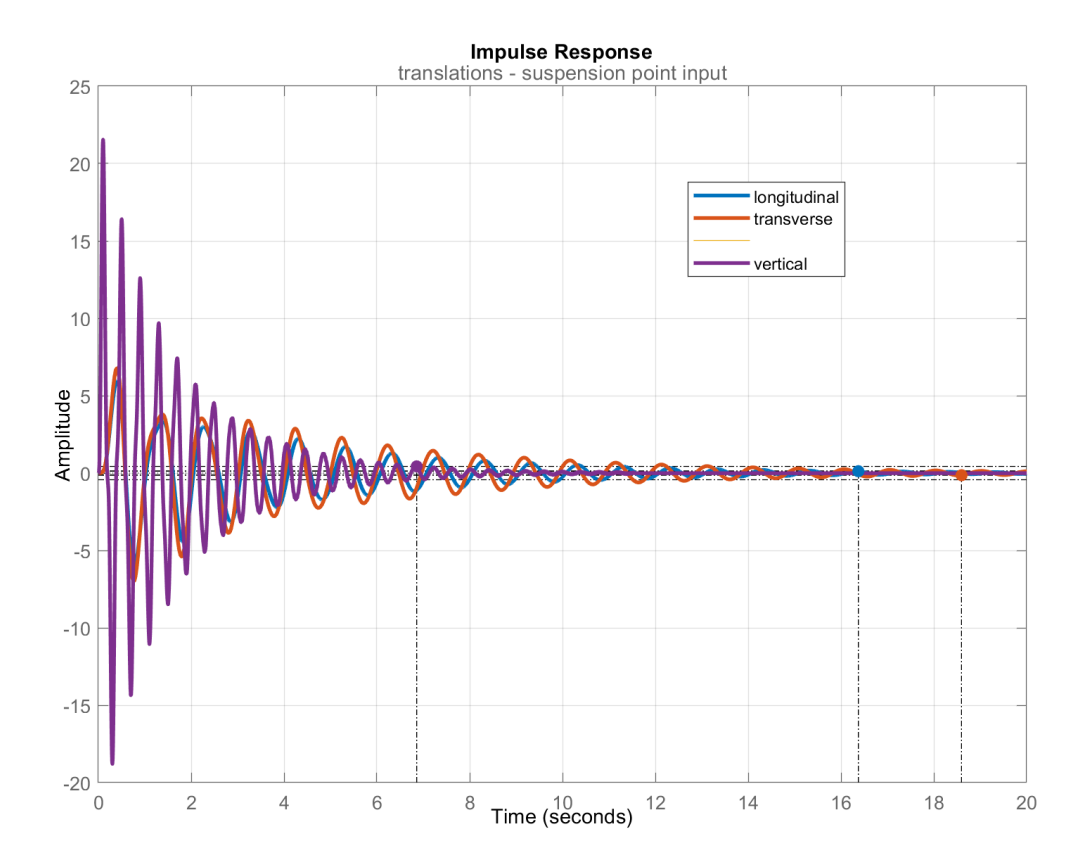


Figure 3: The purple (vertical), blue (longitudinal) and red (transverse-horizontal) curves represent the response to impulses applied at the suspension point as observed at the payload centre-of-mass. The standard settling characteristic is also displayed as a round dot on each curve. In all three cases the lowest-frequency mode dominates.

I/O points to enable transfer functions and impulse responses to be obtained using the 'control-design, linear-analysis' tool. The 'triple model' subsystem contains LTI boxes (lpn, vn, trn, yn) that are the same as in the HSTS model.

Selected MATLAB code is included in small sections below:

```
%% prelims
g = 9.81; %gravitational acceleration
alpha = 1.38; %blade shape factor
ye = 186e9; %Young's elastic modulus for steel blades (revise)
```

Note that the blade parameters are assumed to be approximate, here and below.

```
%% top mass
        = 0.75; %mass from Russell, Feb 19 estimate
m 1
% I1x
           1.76e-3;
                         %moment of inertia (roll) RJ -updated 20
   Feb 19
% I1y
        =
           0.69e-3;
                         %moment of inertia (pitch) RJ -updated 20
    Feb 19
% I1z
        =
           1.63e-3;
                         %moment of inertia (yaw) RJ -updated 20
   Feb 19
% I1x
           2.54e-3;
                         %moment of inertia (roll) AH -updated 22
```

## Impulse Response

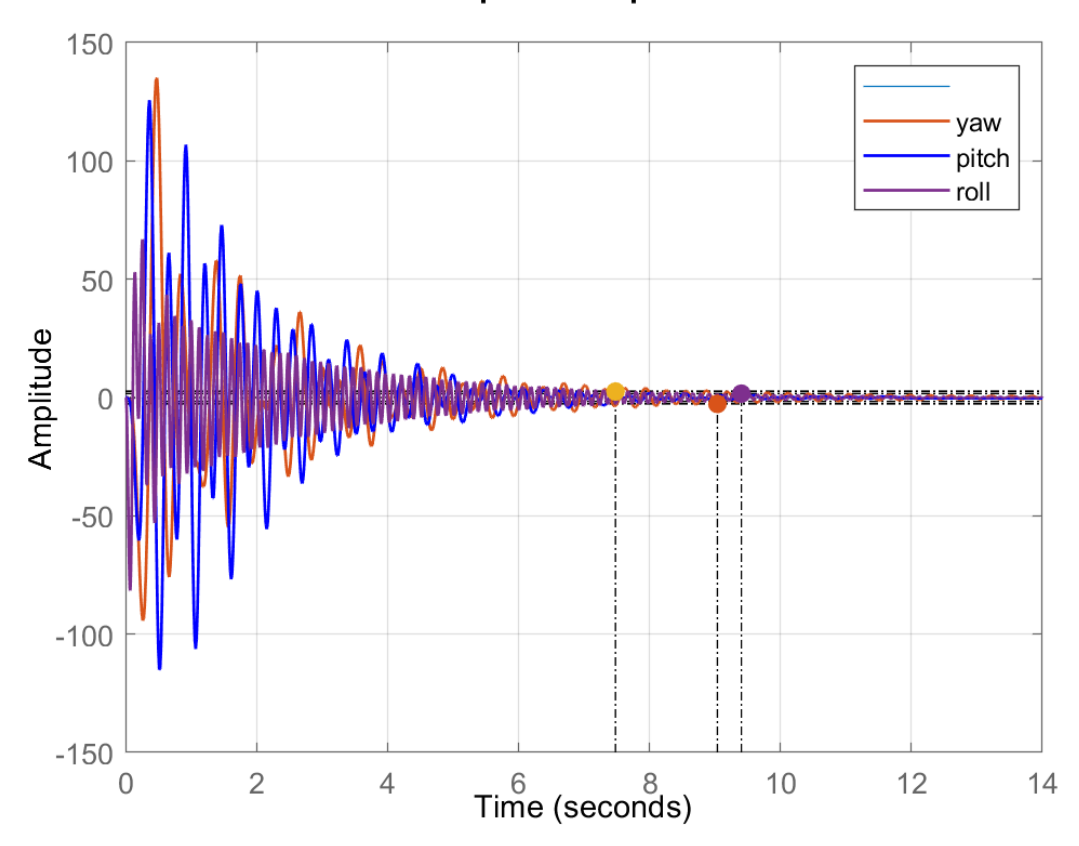


Figure 4: The purple (roll), blue (yaw) and red (pitch) curves represent the response to impulses applied at the relevant sensor input – there is no suspension point input for pitch. Observed at the payload centre-of-mass. The settling characteristic is indicated. The settling time is dominated by the 'middle-frequency' mode in all three cases. This arises from limited coupling between the top mass and the lower two masses. The coupling was increased until a satisfactory outcome was obtained. Further optimisation should be possible by adjustment of the local damping filter.

```
Nov 19
% I1y
           0.673e-3;
                         %moment of inertia (pitch) AH -updated 22
    Nov 19
% I1z
           2.41e-3;
                         %moment of inertia (yaw) AH -updated 22
   Nov 20
                         %moment of inertia (roll) AH -updated 21
I1x
        =
           2.525e-3;
   Feb 20
                         %moment of inertia (pitch) AH -updated 21
           0.6251e-3;
    Feb 20
I1z
           2.435e-3;
                         %moment of inertia (yaw) AH -updated 21
   Feb 20
%
   from AH 25/02/2020
%
                 Matlab Target
                                CAD
                                          Difference
                 1.76E-03
                                 2.525E-03
                                                  -7.654E-04
 Ixx
       (Roll)
   Over by 43.5%
```

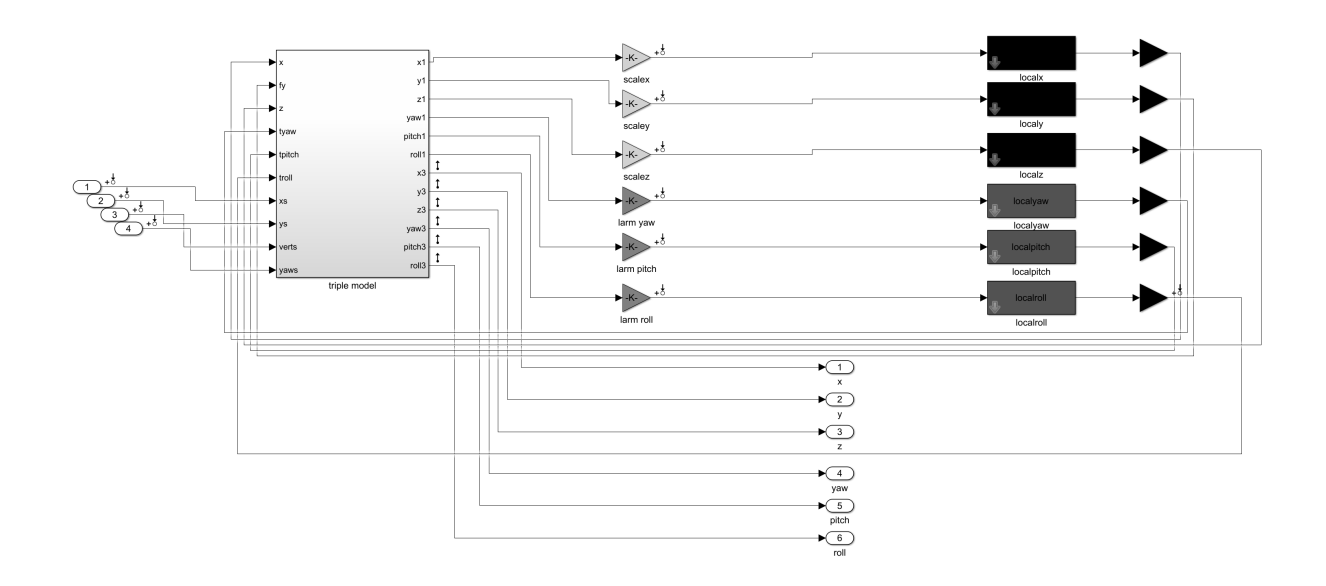


Figure 5: the top-level Simulink diagram as described in the text. Note that the model was prepared with MATLAB release 2018b and is incompatible with much older versions.

```
% Iyy (Pitch) 6.90E-04 6.251E-04 6.495E-05
Under by 9.4%
% Izz (Yaw) 1.63E-03 2.435E-03 -8.051E-04
Over by 49.4%
```

Numbers are from Solidworks, modified to represent design improvements. Revised design has lower I1x and I1y.

```
%% intermediate mass
m2 = 0.802; %RJ -updated 20 Feb
\% I2x = 3.54e-4; \%RJ -updated 20 Feb
% I2y = 6.01e-4; %RJ -updated 20 Feb
\% I2z = 5.73e-4; \%RJ -updated 20 Feb
\% I2x = 3.24e-4; \%AH -updated 22 Nov
% I2y = 6.58e-4;
                  %AH -updated 22 Nov
                  %AH -updated 22 Nov
\% I2z = 6.67e-4;
                      -updated 25 Feb
I2x = 6.874e-4;
                 %AH
12y = 3.677e-4;
                 %AH
                      -updated 25 Feb
I2z = 6.643e-4;
                 %AH
                      -updated 25 Feb
   from AH 25/02/2020
%
                Matlab Target
                               CAD
                                         Difference
% Ixx
       (Roll)
                3.540E-04
                                 6.874E-04
                                                 -3.334E-04
   Over by 94.2%
% Iyy (Pitch)
                6.010E-04
                                 3.677E-04
                                                 2.333E-04
   Under by
                   38.8%
% Izz (Yaw)
                5.730E-04
                                 6.643E-04
                                                 -9.133E-05
   Over by 15.94%
```

These have been revised upward to increase margin for future detail design of top mass.

```
\%\% test mass = payload
            = 0.03; %dimensions of TEST MASS
tх
            = 0.0375;
tr
den3 = 2202; %density (fused silica)
            = den3*pi*tr^2*tx; %test mass
mЗ
I3x
      = m3*(tr^2/2); %moment of inertia (roll)
      = m3*(tr^2/4+tx^2/12); %moment of inertia (pitch)
I3y
I3z
       = m3*(tr^2/4+tx^2/12); %moment of inertia (yaw)
A thicker payload can be accommodated – e.g. up to around 40 mm thick.
%% wire details
           = 0.115;
 11
                       %upper wire length
           = 0.115; %intermediate wire length
 12
           = 0.16; %lower wire length
 13
 nw1
      = 2;
                   % number of wires (= number of cantilevers if
    fitted) per stage (2 or 4)
      = 4;
 nw2
       = 4;
 nw3
            = 52e-6; % radius of upper wire (not critical)
 r1
            = 52e-6; % radius of intermediate wire (not
   critical)
            = 26e-6; % radius of lower wire, FWW measured
   sample (AEI)
  Y1 = 2.12e11; % number as measured by MB, 11/18/05
  Y2 = 2.12e11; % number as measured by MB, 11/18/05
  Y3 = 2.12e11; % number as measured by MB, 11/18/05
%% blade design - upper blades
mtbu = (m1 + m2 + m3)/2; \%total per blade
mbu = m1/2; %uncoupled mass
lbu = 0.12; %blade length
au = 0.018; %blade width
hu = 0.0010; %blade thickness
str1 = 6.*mtbu.*g.*lbu./(au.*hu.^2); %max stress at equilibrium
ufc1 = sqrt(ye.*au.*hu.^3./(4.*mbu.*lbu.^3.*alpha))./2./pi;
intmode1 = 55*hu*0.37^2/(0.002*lbu^2);
defl1u = g/(ufc1*2*pi)^2; %deflection corr. ufc1
defl1=defl1u*mtbu/mbu; %deflection with total load
Predicted stress: str1 = 3.6e+08. Note that the algorithm to estimate blade deflection has
been corrected.
%% blade design - lower blades
mtbl = (m2 + m3)/4; \%total per blade
mbl = m2/4; %uncoupled mass
lbl = 0.065; %blade length
al = 0.012; %blade width
hl = 0.0005; %blade thickness
str2 = 6.*mtbl.*g.*lbl./(al.*hl.^2); %max stress at equilibrium
```

```
ufc2 = sqrt(ye.*al.*hl.^3./(4.*mbl.*lbl.^3.*alpha))./2./pi;
intmode2 = 55*hl*0.37^2/(0.002*lbl^2); %scaled from GEO blade defl2u = g/(ufc2*2*pi)^2; %deflection corr. ufc1 defl2=defl2u*mtbl/mbl; %deflection with total load
```

Predicted stress: str2 = 3.49e+08.

Both sets of blades are indicative, FEA is to be employed to find the correct blade width to yield the desired spring constant while constraining the length and thickness to the above values. This process is expected to result in blades with about the same stress.

```
%% x direction offsets
        = 0.00; % top wires
        = 0.010; % intermediate wires
 si
        = 0.002; % bottom wires
 sl
%% y direction offsets
n0 = 0.030; % top wires at top blades
 n1 = 0.015; % top wires at top mass
n2 = 0.030; % intermediate wires at top mass
 n3 = 0.0405; % intermediate wires at intermediate mass
n4 = 0.0405; % bottom wires at intermediate mass
 n5 = 0.0405; % bottom wires at test mass
%% z direction offsets
 d0 = 0.005;
 d1 = 0.005;
 d2 = 0.003;
 d3 = 0.002;
 d4 = 0.002;
%% Flexure length calcuations and revised d code. Added Aug 2008
   NAR
 c1=sqrt(l1^2-(n1-n0)^2)/l1;
 c2 = sqrt(12^2 - (n3 - n2)^2)/12;
 c3 = sqrt(13^2 - (n5 - n4)^2)/13;
 M11 = (1/4)*pi*r1^4;
 M21 = (1/4)*pi*r2^4;
 M31 = (1/4)*pi*r3^4;
 flex1 = sqrt(nw1*M11*Y1/(m1+m2+m3)/g)*c1^(3/2);
 flex2 = sqrt(nw2*M21*Y2/(m2+m3)/g)*c2^(3/2);
 flex3 = sqrt(nw3*M31*Y3/m3/g)*c3^(3/2);
%% make a controller for each dof
stdgain = -8;
localx = local1(2*stdgain);
localy = local2(2*stdgain);
localz = local3(0.5*stdgain);
```

Note that with assumed degree-of-freedom damping, the larm parameters do not require to be accurate.